

Of Mice and Chickens: Revisiting the RC Time Constant Problem

Kuni H. Iwasa

NIDCD, National Institutes of Health
Bethesda, MD 20892, USA

draft version 3.0: December 14, 2022

running title: *RC roll-off in hair cells*

keywords: *auditory frequencies, electrical resonance, piezoelectric resonance, membrane capacitance*

Abstract

Avian hair cells depend on electrical resonance for frequency selectivity. The upper bound of the frequency range is limited by the RC time constant of hair cells because the sharpness of tuning requires that the resonance frequency must be lower than the RC roll-off frequency. In contrast, tuned mechanical vibration of the inner ear is the basis of frequency selectivity of the mammalian ear. This mechanical vibration is supported by outer hair cells (OHC) with their electromotility based on piezoelectricity, which is driven by the receptor potential. Thus it is also subjected to the RC time constant problem. Association of OHCs with a system with mechanical resonance leads to piezoelectric resonance. This resonance can nullify the membrane capacitance and solves the RC time constant problem for OHCs.

Introduction

Auditory frequencies are extremely high for biological cells, which are subjected to their own intrinsic low-pass filter, often referred to as the RC filter. This filter is due to the combination of the membrane capacitance and the membrane conductance. This filter is characterized by the RC time constant, where R is the membrane resistance and C the membrane capacitance. To overcome this low-pass characteristic of hair cells is a significant challenge for hair cells in the ear. Take mice and chickens, the most commonly used animals for experiments: The auditory range of mice reaches up to 80 kHz [1], that of chickens extends from 0.25 to 4 kHz [2]. The highest among birds is 9 kHz of barn owls [3].

The RC time constant problem has been intensely discussed with respect to outer hair cells (OHCs) in the mammalian ear. OHCs are expected to inject power to the oscillation in the inner ear for the sensitivity and frequency specificity of the mammalian ear [4–6]. However, given the membrane resistance capacitance and membrane resistance of these cells, their RC roll-off frequency is lower than the operating frequency by more than an order of magnitude [7]. This issue, named “RC time constant problem” generated various hypotheses [8–11], including careful re-examination of the membrane resistance [12].

Since all hair cells are subjected to this low pass filter, it is of interest to re-visit this issue, comparing mammalian OHCs with avian hair cells. Biophysical approaches in comparing avian and mammalian hearing would be an interesting addition to more descriptive approaches, such as a parallelism in innervation pattern between avian short hair cells and mammalian OHCs [13].

The present report shows that reduction of the membrane resistance is an effective strategy of elevating the receptor potential at high frequencies in avian hair cells, which primarily depend on electrical resonance for tuning. A recent summary on vertebrate tuning that depends on this mechanism has been presented by Fettiplace [14].

The same strategy does not work for OHCs, which do not have electrical resonance. Instead, OHCs have a significant extra capacitance component, which depend on the membrane potential [15] as well as mechanical load [16]. This component is the key to reduce the total membrane capacitance at the operating frequency [17, 18]. Therefore, avian ears and mammalian ears employ two contrasting strategies for extending the auditory range to high frequencies: reducing the membrane resistance for the former and reducing the membrane capacitance for the latter.

The scope of the present paper is limited to tuning. Generation of neuronal output is not included because it depends on synaptic transmission, which is a separate process not less complicated.

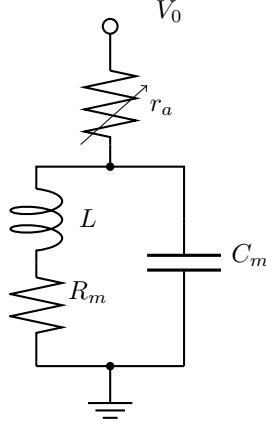


Figure 1: An equivalent circuit for electric resonance. r_a is hair bundle resistance and R_m is cell body resistance. An interplay between Ca^{2+} -channel and Ca^{2+} -activated K^+ channel [20, 22] leads to electrical resonance, which can be represented by a combination of inductance L and capacitance C_m [19].

Avian ears

Electrical resonance has been demonstrated in turtle hair cells [19], frog hair cells [20] and tall hair cells in chicks [21]. The molecular mechanism has been understood as based on the interplay between Ca^{2+} channel and Ca^{2+} -activated K^+ -channel (alias BK channel) [20, 22]. The resonance frequency is associated with the splice variants of the BK channel in the hair cell [23].

From biophysical point of view, the description of electric resonance with Hodgkin-Huxley type equations by including those ion channels would be gratifying. However, such a description involves a good number of parameters [20, 22]. For the purpose of finding the frequency limit of electrical tuning, the number of the parameters should be minimized. For this reason, the equivalent circuit model proposed by Crawford and Fettiplace [19] is advantageous because the electrical properties of hair cells is quite well described with small number of parameters.

Electric resonance

The equivalent circuit proposed by Crawford and Fettiplace is given in Fig. 1. The electrical oscillation, which is realized by an interplay between Ca^{2+} -channel and Ca^{2+} -activated K^+ channel, is introduced by an inductance L .

If the current through the resistor r_a is I , then the basic relationships are,

$$I = I_0 + I_1, \quad (1a)$$

$$I_0 = \frac{dQ_0}{dt}, \quad Q_0 = CV \quad (1b)$$

$$V = \left(R + L \frac{d}{dt} \right) I_0 \quad (1c)$$

These relationships lead to

$$LC \frac{d^2 V}{dt^2} + RC \frac{dV}{dt} + V = RI + L \frac{dI}{dt}. \quad (2)$$

Now input sinusoidal current $I = \langle I \rangle + i_{\text{in}} \exp[i\omega t]$, and let $V = \langle V \rangle v \exp[i\omega t]$. Then the differential equation turns into

$$(-\bar{\omega}^2 + i\bar{\omega}/\bar{\omega}_{rc} + 1)v = (R + i\omega L)i_{\text{in}} \quad (3)$$

where

$$\bar{\omega} = \omega/\omega_r, \quad \omega_r^2 = 1/(LC), \quad (4a)$$

$$\bar{\omega}_{rc} = \omega_{rc}/\omega_r, \quad \omega_{rc} = 1/(RC). \quad (4b)$$

A larger value for the RC roll-off frequency $\bar{\omega}_{rc}$ gives rise to a sharper resonance peak. For this reason, it is known as the quality factor Q . Eqs. 4 indicates that the ratio L/R can be expressed by ω_{η}/ω_r^2 . Thus, Eq. 3 can be expressed by

$$(-\bar{\omega}^2 + i\bar{\omega}/\bar{\omega}_{rc} + 1)v = R(1 + i\bar{\omega} \cdot \bar{\omega}_{rc})i_{\text{in}}. \quad (5)$$

The resulting tuning curve is shown in Fig. 2. A frequency dependent term in the nominator somewhat affects the outcome but the difference is not very large. The existence of a peak frequency requires the condition $\bar{\omega}_{rc} > 1$.

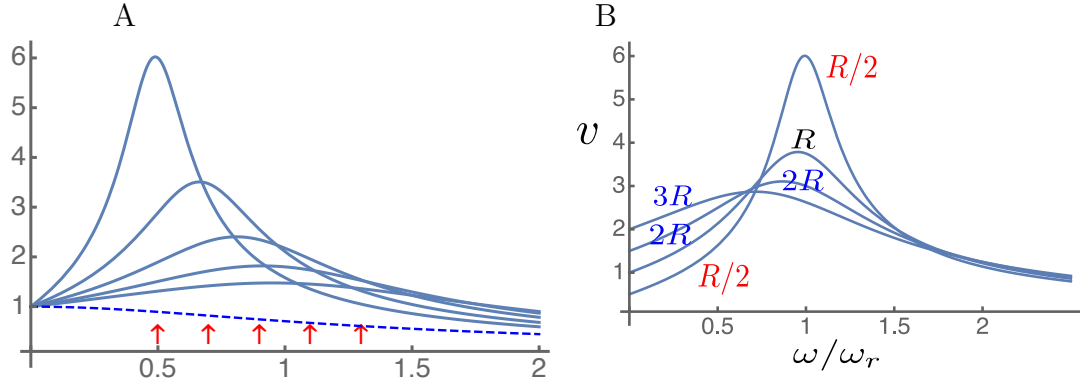


Figure 2: The effect of resonance frequency and RC roll-off frequency on the amplitude v of the receptor potential (Eq. 8). The amplitude v is normalized at $\omega = 0$. A: The effect of changing the resonance the ratio ω_{rc} . The frequency axis is normalized by the RC roll-off frequency ω_{rc} . The values for ω_r/ω_{rc} are 0.5, 0.7, 0.9, 1.1, and 1.3 (red arrows). The broken line shows the response without resonance. The value of R is set to unity. B: The effect of the membrane resistance R . The frequency axis is normalized by the resonance frequency. Relative values r of the membrane resistance R are 0.5, 1, 1.5 and 2, standardizing $\omega_{rc}/\omega_r = 1.5$ at $R = 1$.

Now, current input I is due to changes in the hair bundle resistance r_a , expressed by

$$I = (V_0 - V)/r_a \quad \text{with} \quad (6a)$$

$$r_a = \langle r_a \rangle (1 - r \exp[i\omega t]). \quad (6b)$$

If the relative change in the hair bundle resistance r is small, we obtain

$$I \approx \langle I \rangle + \left(\langle I \rangle r - \frac{v}{\langle r_a \rangle} \right) \exp[i\omega t],$$

where $\langle I \rangle = (V_0 - \langle V \rangle) / \langle r_a \rangle$. Thus, we obtain

$$i_{\text{in}} = \langle I \rangle r - \frac{v}{\langle r_a \rangle} \quad (7)$$

Thus Eq. 5 is replaced by

$$\left(-\bar{\omega}^2 + i\bar{\omega} \left(\frac{1}{\bar{\omega}_{rc}} + \bar{\omega}_{rc} \frac{R}{\langle r_a \rangle} \right) + 1 + \frac{R}{\langle r_a \rangle} \right) v = \langle I \rangle R (1 + i\bar{\omega} \cdot \bar{\omega}_{rc}) r, \quad (8)$$

The frequency dependence approaches the case of sinusoidal input current (Eq. 5) if $R/\langle r_a \rangle \rightarrow 0$, as would be expected. That is indeed the physiological condition.

The above equations show that the efficacy of electric tuning requires that ω_η , the roll-off frequency of the RC filter, must be higher than the resonance frequency ω_r . In other words, the roll-off frequency of the intrinsic RC filter dictates the frequency bandwidth.

Control by membrane resistance

The membrane capacitance depends on the surface area. Tall hair cells on the neural side of the chicken basal papilla do not show much difference in apparent membrane area [24] and indeed in the membrane capacitance measured [21].

A reduction of the membrane resistance to enhance the receptor potential may appear counterintuitive because that reduces the receptor potential in the low frequency range (Fig. 2B). However, this effect can sharply enhance the receptor potential near the resonance frequency because it elevates the RC roll-off frequency (Fig. 2B). The net gain near the resonance frequency more than compensates for the reduction due to the decreased R_m .

This strategy of reducing the membrane resistance R_m is, unlike reducing the membrane capacitance C_m , not physically constrained. However, it could be metabolically taxing. To achieve an RC roll-off frequency of 10 kHz, R_m must be ~ 2 M Ω . In addition, electrical resonance itself requires higher metabolic rates for high frequencies because the resonance mechanism requires oscillation of intracellular Ca^{2+} ion concentration. Oscillation of intracellular Ca^{2+} ion concentration during each cycle means a higher rate of calcium extrusion to operate at higher frequencies.

Since the resonance frequency must be lower than the RC roll-off frequency, even with a roll-off frequency of 10 kHz, the reasonably sharp resonance must be $(10/Q)$ kHz, where Q is the value of the quality factor. To achieve quality factor 5, the value common for turtle hair cells [19], the resonance frequency must be 2 kHz. For this reason, achieving the upper limit of 4 kHz for the chicken may require an additional mechanism.

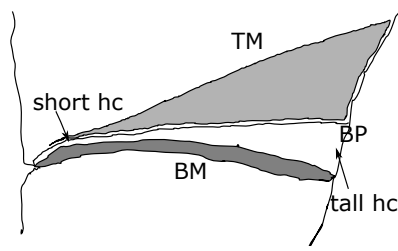


Figure 3: The cross-section of the avian inner ear. TM: the tectorial membrane, BM: the basilar membrane, BP: the basilar papilla. After Gleich and Manley[25].

Motion of tectorial membrane

A mechanism that can enhance high-frequency hearing could be based on the tonotopic organization of the avian ear. One such mechanism could be the movement of the tectorial membrane (TM). The avian TM, which is softer than the mammalian one, is tapered toward the abneural side (Fig. 3) and the tapering increases toward the base.

Like OHCs in the mammalian ear, short hair cells are located nearly above the middle of the basilar membrane, the movement of which in the up-down direction [26] would effectively transmit bending stress to the short hair cells' hair bundles. In contrast, tall hair cells, which function as the sensor, are located away from the center of the basilar membrane, at a location seemingly unsuitable for sensing the motion of the basilar membrane directly. Thus it is likely short hair cells are involved in amplification by a hair bundle active process [27–30], transmitting the mechanical vibration of the basilar membrane to the hair bundles of tall hair cells. The problem is how that can happen? To address this question, it requires to identify the vibrational mode, which involves the basilar membrane, the basilar papilla, and the TM.

Since hair cell bundles are stimulated by bending, it would be logical to assume that shear motion between the basilar papilla and the TM stimulates the hair bundles. Although the orientation of hair bundles forms domain structure in a more apical region, it is uniform in the basal region [25, 31]. In the following, we examine the mode of motion that is consistent with the bundle alignment in the basal area, then consider a possible mechanism for domain formation in the more apical region. For describing the tapering of the TM, two-mass models are used (Fig. 4). One has a smaller mass m , located at the top of short hair cells and another with a larger mass M , located at the top of tall hair cells [32].

The small mass m is connected to the larger mass M with a spring with stiffness k and the larger mass M is connected with the wall by another spring with stiffness K . Let X the displacement of the bigger mass from its equilibrium position, and that of smaller one be x . Let η_2 be viscous drag on mass M and η_1 be negative drag on mass m to mimic the amplifying role of short hair cells

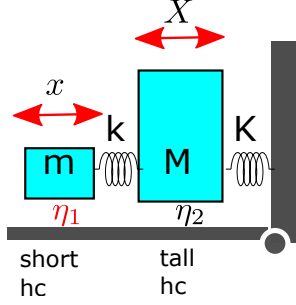


Figure 4: A possible mode of motion of the avian inner ear. Two squares represent two parts of the tectorial membrane. The smaller one on top of short hair cells and the larger one on top of tall hair cells. The tapering the tectorial membrane is represented by the mass ratio M/m .

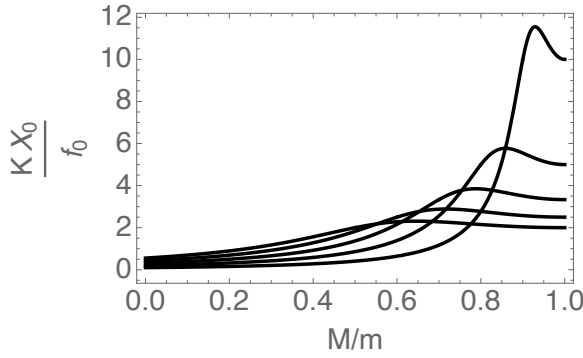


Figure 5: Force amplitude KX_0/f_0 , normalized to that of the driving external force, applied to the mass M at $\omega = \omega_0$, is plotted against the mass ratio M/m . The reduced drag coefficient $\bar{\eta} = \eta/(M\omega_0)$ ranges from 0.1 to 0.5 incremented by 0.1. The peak is at small values of mass ratio M/m for the small value of $\bar{\eta}$ and systematically shifts to larger values as $\bar{\eta}$ increases.

(Fig. 4 A). The set of equations is given by,

$$\left(m \frac{d^2}{dt^2} - \eta_1 \frac{d}{dt}\right) x - k(X - x) = f_0 \exp[i\omega t] \quad (9)$$

$$\left(M \frac{d^2}{dt^2} + \eta_2 \frac{d}{dt} + K\right) X - k(X - x) = 0, \quad (10)$$

where $f_0 \exp[i\omega t]$ is a periodic external force of angular frequency ω applied to mass m , which is located just above the center of the basilar membrane. Here it is assumed that up-down motion of the basilar membrane results in this external force. Following Steele [27], let ω_0 be the resonance frequency of the tectorial membrane, i.e. $\omega_0^2 = K/M = k/m$ and seek a steady state solution.

The force applied to the mass M is plotted for a special case of $\eta_1 = \eta_2 = \eta$ (Fig. 5A). For a given value of M , this force is larger for smaller values of the reduced drag $\bar{\eta}$ where the ratio m/M is smaller. Since the reduced drag is defined by $\bar{\eta} = \eta/(M\omega_0)$, this parameter is smaller for higher frequency ω_0 . Thus the plot shows that the force is maximal for large ratio M/m at larger frequencies. This result is consistent with the experimental finding that the sharpness of tapering of the TM increases from the apical to the basal end [31, 33]. One can argue that the force relevant to the transduction of tall hair cells would be better related to drag $\eta dX/dt$ rather than the force KX_0 . That does not change the optimal mass ratio because drag is represented by $\bar{\eta} KX_0$, maximizing at the same mass ratio. The condition for resonance is not very strict because those peaks exist for $1 \leq \omega/\omega_0 \leq 1.4$.

Motion of the tectorial membrane, however, has not been detected [34]. The major difficulty in observing such motion is in the low optical density of the avian tectorial membrane, which lacks collagen. In addition, the border between the tectorial membrane and the basilar papilla could be optically blurry. Unlike the flat surface of the mammalian tectorial membrane, the avian TM has an elaborate structure on the side facing the basilar papilla. A thin veil-like structure descends to the basilar papilla, surrounding each hair cell [35]. A dome like recess above each hair cell and each hair bundle makes contact with the tectorial membrane at the dome [35].

Mammalian ears

Mature mammalian cochlear hair cells, neither inner hair cells (IHCs), nor OHCs (OHCs), show spontaneous firing or electrical oscillation. The organ of Corti, into which hair cells are incorporated, shows marked displacements, which are associated with the traveling wave on the basilar membrane, during acoustic stimulation of the ear [36].

Outer hair cell motility has been thought to provide power into the motion in the cochlea to amplify the oscillation in the organ of Corti [4, 5]. However, the frequency dependence of such a function had been a puzzle, often referred to as “RC time constant problem,” which many investigators tried to solve [8–12, 17, 37–40]. The reason was that the roll-off frequencies of OHCs are much lower than their operating frequencies and such a discrepancy appeared to makes the physiological role of these cells unlikely.

Two components of the capacitance

A puzzle for evaluating the RC time constant is the value of the membrane capacitance to use because OHCs have two major components of their membrane capacitance. One of the components has been referred to as the “regular capacitance.” It does not depend on the membrane potential, quite similar to the membrane capacitance of most cells. Indeed, it is consistent with the standard specific capacitance of $1\mu\text{F}/\text{cm}^2$ [41]. The other main component is often called “nonlinear capacitance” because it shows a bell-shaped dependence on the membrane potential [15, 42]. It is associated with prestin [43], a member of the SLC family of membrane proteins, which confers voltage-dependent motility on OHCs [5], often referred to as electromotility. For the purpose of clarifying the origins, let us call the former the “structural” capacitance, and the latter “prestin” capacitance.

Prestin capacitance cannot be ignored because at its peak voltage it is larger than the structural capacitance in basal OHCs. It shows frequency dependence [44] and sensitivity to mechanical force and constraints [16, 45, 46], consistent with mechanoelectric coupling, or piezoelectricity, of this molecule [47].

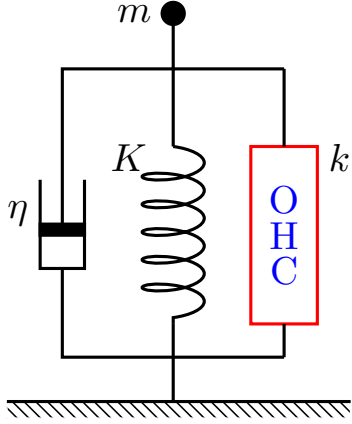


Figure 6: OHCs incorporated into a mechanically resonating system. A schematic diagram (left) and the resulting frequency-dependent (or nonlinear) component C_p of the membrane capacitance (right). In the schematic diagram, K is the stiffness of the elastic load, η the drag coefficient, and m the inertial mass. The intrinsic stiffness of the OHC is k . In the plot, $\bar{\omega} = \omega/\omega_r$, where the resonance frequency ω_r is determined by $\omega_r^2 = (k + K)/m$.

Piezoelectric resonance

OHCs undergo reduction of their length in response to depolarization and elongation in response to hyperpolarization. Inversely, externally imposed length changes of OHCs induce membrane current, consistent with piezoelectricity [47].

For this reason, if OHCs are associated with a mechanically resonating system, piezoelectric resonance is expected. At frequencies lower than resonance point, the electric charge in prestin moves in phase with the rest of capacitor charge, which is by 90 degrees in advance of the voltage waveform. Near the mechanical resonance frequency of the system, the mechanical oscillation together with the length changes of the OHC is delayed by 90 degrees from the voltage waveform. Under this condition, the current carried by prestin goes opposite of the capacitor current, reducing or even reversing the total current, resulting in reduced or negative capacitance, depending on the relative significance of the charge of the motile element. This is equivalent to piezoelectric resonance and the motile membrane protein pumps electrical energy into mechanical vibration without being hindered by the RC time constant problem, as described below.

A model system

In the following, a brief account of such an oscillator system is given. A more detailed descriptions are available [17, 18]. Let an OHC incorporated into a system with mechanical resonance as illustrated in Fig. 6. In the following, piezoelectric resonance is described, focusing the membrane capacitance. The description largely follows the one-dimensional model [17], rather than the more realistic cylindrical model [18] for simplicity.

motile element

Let a motile element in the lateral membrane of the OHC has two states, the long state L and the short state S, and let P the fraction of the motile element in state L. The natural length of the cell would be $X_0 + anP$, where a is the contribution of a single motile element to the cell length accompanied by

conformational change from S to L. The same conformational change transfer charge q across the membrane. The quantify n is the number of the motile elements in the cell.

In the existence of the elastic load K , the displacement X due to the motile unit is given by

$$X = anP k/(k + K), \quad (11)$$

where k is the structural stiffness of the cell. In addition, assume that P_∞ at equilibrium follows the Boltzmann distribution

$$P_\infty/(1 - P_\infty) = \exp[-\beta(G_0 + qV + aF_o)] \quad (12)$$

where $\beta = 1/(k_B T)$ with Boltzmann's constant k_B and the temperature T . The constant term is represented by G_0 . The quantities V and F_o are, respectively, the membrane potential and force applied from the external elastic load, which is associated with axial displacement X of the cell. Since the stiffness of the external elastic load is K , $F_o = KX$.

equation of motion

The equation of motion of the system that is illustrated in Fig. 6 can be expressed by

$$m d^2X/dt^2 + \eta dX/dt = k(X_\infty - X), \quad (13)$$

where $X_\infty = anP_\infty k/(k + K)$ is the displacement that corresponds to equilibrium, m is the mass, and η drag coefficient. The inertia term can be justified if the system is not far from equilibrium [18]. The difference between the current displacement X and equilibrium displacement X_∞ is the driving force. The equation of motion (13) can be expresses using variable P

$$m d^2P/dt^2 + \eta dP/dt = (k + K)(P_\infty - P). \quad (14)$$

prestin capacitance

Now consider the response to a sinusoidal voltage waveform of small amplitude v and angular frequency ω . Let p the corresponding small amplitude of P .

$$V = V_0 + v \exp[i\omega t], \quad P = P_0 + p \exp[i\omega t].$$

Then the equation of motion (14) is transformed into

$$p = \frac{-\gamma q}{-\bar{\omega}^2 + i\bar{\omega}/\bar{\omega}_\eta + \alpha^2} v, \quad (15)$$

where $\bar{\omega}(= \omega/\omega_r)$ is the frequency normalized to the mechanical resonance frequency $\omega_r = \sqrt{(k + K)/m}$, $\bar{\omega}_\eta$ is normalized viscoelastic roll-off frequency,

$\gamma = \beta P_0(1 - P_0)$, and $\alpha^2 = 1 + \gamma a^2 n k K / (k + K)$. The coefficients γ and α originate from the expansion of the exponential term of P_∞ .

The contribution C_p of the movement of prestin charge to membrane capacitance can be obtained from $C_p = (nq/v) \text{Re}[p]$, where $\text{Re}[\dots]$ indicates the real part. This results in

$$C_p = \frac{\gamma n q^2 (\alpha^2 - \bar{\omega}^2)}{(\alpha^2 - \bar{\omega}^2)^2 + (\bar{\omega}/\bar{\omega}_\eta)^2}. \quad (16)$$

Notice here that $C_p < 0$ where $\bar{\omega} > \alpha$ is satisfied. Since the parameter α^2 is only a little larger than unity for the most cases, C_p is negative for the frequency region from near the resonance frequency and higher (Fig. 7).

The total membrane capacitance C_m is the sum of the structural capacitance C_0 and prestin capacitance C_p , i.e. $C_m = C_0 + C_p$. This might appear that a small value of C_0 is favorable to achieve the condition $C_m \rightarrow 0$. However, that is not that simple because a shorter OHC with smaller C_0 may have smaller number n of prestin, which determines the significance of C_p .

For this reason, it is necessary to examine how C_0 affects the optimal power production of the OHC with hair bundle stimulation.

response to hair bundle stimulation

The effect of hair bundle resistance R_a on the membrane potential V can be expressed

$$(e_{ec} - V)/R_a = (V - e_K)/R_m + C_0 dV/dt - nq dP/dt, \quad (17)$$

where e_{ec} is the endocochlear potential, e_K is the resting potential of OHC, which is primarily determined by K^+ conductance, and R_a hair bundle conductance.

If we assume that stimulation at the hair bundle is periodic with angular frequency ω , introducing the time independent component R_0 and the relative amplitude r of the hair bundle resistance R_a , we obtain

$$-i_0 r = (\sigma + i\omega C_0)v - i\omega nqp. \quad (18)$$

Here $i_0 = (e_{ec} - e_K)/(R_0 + R_m)$ is the steady state current and $\sigma = 1/R_0 + 1/R_m$ the steady state conductance, which can be dropped for high frequency stimulation because it is smaller than ωC_0 .

From the transformed equation of motion Eq. 15 and equation for receptor potential Eq. 18, p can be expressed as a linear function of r .

$$p(-\bar{\omega}^2 + i\bar{\omega}/\bar{\omega}_\eta + \alpha^2 + \zeta) = -\frac{\gamma i_0 q}{\omega C_0} r, \quad (19)$$

where $\zeta = \gamma n q^2 / C_0$, which is the ratio of prestin capacitance at the zero-frequency limit to the structural capacitance. The equation shows that the

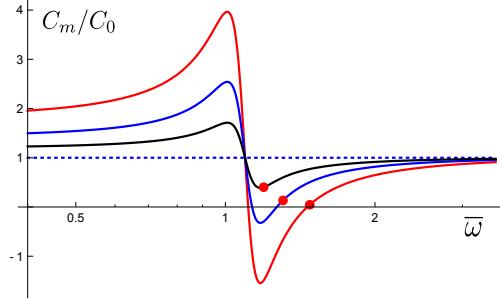


Figure 7: Negative membrane capacitance due to motile charge. Motile charge produces negative capacitance near resonance frequency, capable of eliminate the structural membrane capacitance C_0 . At the frequencies of maximal power generation by an OHC, which are marked by filled red circles, the total membrane capacitance is slightly positive, as indicated by Eq. 20.

damping term $1/\bar{\omega}_\eta = \omega_r/\omega_\eta$ must be small not to be overdamped. Notice also that $|p|$ is inversely proportional to C_0 .

To evaluate the power output of the OHC, only the work against drag during a half-cycle is $E_d = (1/2)\eta\omega k^2|anp|^2/(k+K)^2$. The work against elastic load does not need to be considered because it is recovered during every cycle. Power output is $Wd = (\omega/\pi)E_d$. Since p is inversely proportional to the structural capacitance C_0 , small C_0 is advantageous for power output.

membrane capacitance

Under the condition of maximal power output, the total membrane capacitance can take an approximate form [17]

$$\begin{aligned} C_m &= C_0 + C_p \\ &\approx C_0 \frac{2\alpha^2 + \zeta}{2\zeta^2} \left(\frac{\omega_r}{\omega_\eta} \right)^2 \end{aligned} \quad (20)$$

Notice that the membrane capacitance is proportional to C_0 and is small if $\omega_r/\omega_\eta < 1$ (Fig. 7).

The diminishing value of the membrane capacitance near the resonance frequency solves the RC time constant problem in OHCs. Therefore, the receptor potential of OHCs in this frequency range is not attenuated, even though it is not enhanced because electrical resonance is absent unlike avian hair cells. Enhancement is in the amplitude of the motion associated with OHCs. This, in turn, results in tonotopic stimulation of IHCs, which generates significant rise in the DC component of their receptor potential at high frequencies.

Discussion

The RC time constant problem for high frequency hearing is shared by hair cells of all ears. The solution differs in avian ears and mammalian ears.

Avian hair cells

Electrical resonance, which functions as the tuning mechanism in non-mammalian hair cells are, subjected to the frequency limit, which is imposed by the low-pass RC filter of their intrinsic electric circuit, which is determined by the membrane capacitance and membrane conductance.

The presence of prestin is not limited to mammalian hair cells. It is also present in avian hair cells and its role in active bending of their stereocilia has been reported [48]. However, its contribution to the membrane capacitance is up to 20 fF/pF, two orders of magnitude smaller than the structural capacitance [48]. For this reason, avian prestin unlikely has any significant effect in reducing the membrane capacitance of the avian hair cells.

Membrane area

Short hair cells occupy larger areas than tall hair cells do on the basilar papilla. Among tall hair cells, basal hair cells take larger areas than apical cells do [25, 49]. Since basal cells are shorter than apical cells, the comparison of their total membrane area is not as certain. Crude estimate from published cell outlines [25]) can be made assuming cylindrical shape for apical cells and top-truncated conical shape for basal cells. Such an attempt leads to somewhat (about 10 to 30%) larger membrane areas for basal cells. However, measured values for the membrane capacitance are about the same [21].

Therefore, the range of the RC roll-off frequency that enables the auditory range of chickens must be accomplished by about 20-fold decrease in the membrane resistance R_m from apical to basal hair cells as described in the earlier section. The low membrane resistance R_m in basal cells may require a larger metabolic rate to operate. In addition, electrical resonance involves oscillatory intracellular Ca^{2+} concentration requires Ca^{2+} removal. This metabolic constraint is consistent with the finding that the predominant metabolism of basal hair cells is oxidative as opposed to glycolytic in apical hair cells that operates at lower frequencies [50].

Other birds

Of avian ears, two groups, songbirds and owls, show auditory ranges and sensitivities, which are different from chickens [51]. These differences are reflected in the hair cell morphology. In barn owls, which have much larger auditory range and sensitivity, basal hair cells are much smaller than apical hair cells [52]. Nonetheless the membrane resistance also plays the dominant role in determining the RC roll-off frequency because difference in the membrane area is much less than the auditory range. The ratio of the surface area of the most apical tall hair cells to the most basal hair cells is about 5:1 if the surface area can be estimated from the cell outline assuming axial symmetry (Fig. 2 of Ref. [52]). The auditory range is from 0.1 kHz to 9 kHz [3, 52], much wider than the area ratio can accommodate.

Mammalian OHC

Traveling wave proceeds from the basal end toward the apical end of the cochlea. This means energy flow accompanied by traveling wave may contribute to the local energy balance in general but energy influx is absent the basal part where the wave initiates. In other words, the condition for local energy balance involving resonance can be considered as a necessary condition for upper bound of the auditory frequency as described above.

Piezoelectric resonance

Mammalian OHCs can overcome the limitation by significantly reducing the membrane capacitance with piezoelectric resonance, as the result of piezoelectric property of prestin in OHCs and mechanical resonance in the cochlea [17, 18]. The residual membrane capacitance is proportional to the structural membrane capacitance C_0 , and the maximal power output of OHC is inversely proportional to C_0 . Therefore the surface area must be small to operate at high frequencies consistent with morphological observations [53].

Analogous to avian hair cells, basal OHCs do have smaller basolateral resistance [12]. This finding appears as if lower membrane resistance R_m can elevate the RC roll-off frequency. It should be noticed, however, reduction of the membrane resistance R_m only reduced the receptor potential in OHCs unlike avian hair cells. This appears to match the larger hair bundle conductance of the basal cells [54].

The auditory ranges

Elevating the RC roll-off frequency to the high end of the auditory frequencies by reducing the membrane resistance appears to have a limit. Even for chickens, the auditory range of which is up to 4 kHz, the reception of the upper end is aided by the tonotopic organization of the inner ear, including the tectorial membrane. For mammalian ears, the auditory range of which extends to 40 kHz and beyond, elevating the RC roll-off frequency by decreasing membrane resistance does not appear practical. In addition, no gain in the receptor potential because these cells do not have electric resonance. The only possible way of solving the RC constant problem is to reduce the membrane capacitance. That can be accomplished by using piezoelectric resonance.

Acknowledgments

I thank Dr. Catherine Weisz of NIDCD for reading an earlier version. This research was supported in part by the Intramural Research Program of the NIH, NIDCD.

References

1. Ehret, G., 1976. Development of absolute auditor thresholds in the house mouse (*Mus musculus*). *J. Am. Audiol. Soc.* 1:179–184.
2. Rebillard, G., and E. W. Rubel, 1981. Electrophysiological study of the maturation of auditory responses from the inner ear of the chick. *Brain Res.* 229:15–23.
3. Sullivan, W. E., and M. Konishi, 1987. Segregation of stimulus phase and intensity coding in the cochlear nucleus of the barn owl. *J. Neurosci.* 4:1787–1799.
4. Brownell, W., C. Bader, D. Bertrand, and Y. Ribaupierre, 1985. Evoked mechanical responses of isolated outer hair cells. *Science* 227:194–196.
5. Ashmore, J. F., 1987. A fast motile response in guinea-pig outer hair cells: the molecular basis of the cochlear amplifier. *J. Physiol.* 388:323–347.
6. Dallos, P., X. Wu, M. A. Cheatham, J. Gao, J. Zheng, C. T. Anderson, S. Jia, X. Wang, W. H. Y. Cheng, S. Sengupta, D. Z. Z. He, and J. Zuo, 2008. Prestin-based outer hair cell motility is necessary for mammalian cochlear amplification. *Neuron* 58:333–339.
7. Housley, G. D., and J. F. Ashmore, 1992. Ionic currents of outer hair cells isolated from the guinea-pig cochlea. *J. Physiol.* 448:73–98.
8. Dallos, P., and B. N. Evans, 1995. High-frequency outer hair cell motility: corrections and addendum. *Science* 268:1420–1421.
9. Mistrík, P., C. Mullaley, F. Mammano, and J. Ashmore, 2009. Three-dimensional current flow in a large-scale model of the cochlea and the mechanism of amplification of sound. *J R Soc Interface* 6:279–291. <http://dx.doi.org/10.1098/rsif.2008.0201>.
10. Spector, A. A., W. E. Brownell, and A. S. Popel, 2003. Effect of outer hair cell piezoelectricity on high-frequency receptor potentials. *J Acoust Soc Am* 113:453–461.
11. Rabbitt, R. D., S. Clifford, K. D. Breneman, B. Farrell, and W. E. Brownell, 2009. Power efficiency of outer hair cell somatic electromotility. *PLoS Comput. Biol.* 5:e1000444. <http://dx.doi.org/10.1371/journal.pcbi.1000444>.
12. Johnson, S. L., M. Beurg, W. Marcotti, and R. Fettiplace, 2011. Prestin-driven cochlear amplification is not limited by the outer hair cell membrane time constant. *Neuron* 70:1143–1154.

13. Köppl, C., 2015. Chapter 6. Avian hearing. *In* C. G. Sacnes, editor, Sturkie's Avian Physiology (6th edition), Academic Press, 71–87.
14. Fettiplace, R., 2020. Diverse Mechanisms of Sound Frequency Discrimination in the Vertebrate Cochlea. *Trends Neurosci.* 43:88–102.
15. Santos-Sacchi, J., 1991. Reversible inhibition of voltage-dependent outer hair cell motility and capacitance. *J. Neurophysiol.* 11:3096–3110.
16. Adachi, M., and K. H. Iwasa, 1999. Electrically driven motor in the outer hair cell: Effect of a mechanical constraint. *Proc. Natl. Acad. Sci. USA* 96:7244–7249.
17. Iwasa, K. H., 2017. Negative membrane capacitance of outer hair cells: electromechanical coupling near resonance. *Sci. Rep.* 7:12118.
18. Iwasa, K. H., 2021. Kinetic membrane model of outer hair cells. *Biophys. J.* 120:122–132.
19. Crawford, A. C., and R. Fettiplace, 1981. An electrical tuning mechanism in turtle cochlear hair cells. *J. Physiol.* 312:377–412.
20. Hudspeth, A. J., and R. S. Lewis, 1988. A model for electrical resonance and frequency tuning in saccular hair cells of the bull-frog, *Rana Castebeliana*. *J Physiol.* 400:275–297.
21. Fuchs, P. A., T. Nagai, and M. G. Evans, 1988. Electrical tuning in hair cells isolated from the chick cochlea. *J Neurosci* 8:2460–2467.
22. Wu, Y.-C., J. J. Art, M. B. Goodman, and R. Fettiplace, 1995. A kinetic description of the Calcium-activated potassium channel and its application to electrical tuning of hair cells. *Prog. Biophys. Molec Biol.* 63:131–158.
23. Jones, E. M. C., C. Laus, and R. Fettiplace, 1998. Identification of Ca^{2+} -activated K^{+} channel splice variants and their distribution in the turtle cochlea. *Proc. Roy. Soc. Lond. B* 265:685–692.
24. Gleich, O., and G. A. Manley, 2000. The hearing organ of birds and crocodilia. *In* R. J. Dooling, R. R. Faye, and A. N. Popper, editors, Comparative Hearing: Birds and Reptiles, Springer, New York, NY, 70–138.
25. Gleich, O., and G. A. Manley, 2000. The hearing organ of birds and crocodilia. *In* R. J. Dooling, R. R. Fay, and P. A. N., editors, Comparative Hearing: Birds and Reptiles, Springer, New York, 70–138.
26. Gummer, A. W., J. W. Smolders, and R. Klinke, 1987. Basilar membrane motion in the pigeon measured with the Mössbauer technique. *Hear Res* 29:63–92.

27. Steele, C. R., 1997. Three-dimensional mechanical modeling of the cochlea. *In* E. R. Lewis, G. R. Long, R. F. Lyon, P. M. Narins, C. R. Steele, and E. Hecht-Poinar, editors, *Diversity in Auditory Mechanics*, World Scientific, Singapore, 455–461.
28. Choe, Y., M. O. Magnasco, and A. J. Hudspeth, 1998. A model for amplification of hair-bundle motion by cyclical binding of Ca^{2+} to mechanoelectrical-transduction channel. *Proc. Natl. Acad. Sci. USA* 95:15321–15326.
29. Tinevez, J.-Y., F. Jülicher, and P. Martin, 2007. Unifying the various incarnations of active hair-bundle motility by the vertebrate hair cell. *Biophys J* 93:4053–4067.
30. Sul, B., and K. H. Iwasa, 2009. Amplifying effect of a release mechanism for fast adaptation in the hair bundle. *J Acoust Soc Am* 126:4–6. <http://dx.doi.org/10.1121/1.3143782>.
31. Köppl, C., O. Gleich, G. Schwabedissen, E. Siegl, and G. A. Manley, 1998. Fine structure of the basilar papilla of the emu: implications for the evolution of avian hair-cell types. *Hear Res* 126:99–112.
32. Iwasa, K. H., and A. J. Ricci, 2015. The avian tectorial membrane: Why is it tapered. *In* K. D. Karavitaki, and D. P. Corey, editors, *Mechanics of Hearing: Protein to Perception*, American Institute of Physics, Melville, NY, 08005.1–08005.6. <http://dx.doi.org/10.1063/1.4939396>.
33. Smith, C. A., M. Konishi, and N. Schuff, 1985. Structure of the barn owl’s (*Tyto alba*) inner ear. *Hear Res* 17:237–247.
34. Xia, A., X. Liu, P. D. Raphael, B. E. Applegate, and J. S. Oghalai, 2016. Hair cell force generation does not amplify or tune vibrations within the chicken basilar papilla. *Nature Commun.* 12133.
35. Goodyear, R., M. Holley, and G. Richardson, 1994. Visualisation of domains in the avian tectorial and otolithic membranes with monoclonal antibodies. *Hear Res* 80:93–104.
36. Békésy, G. v., 1952. DC resting potentials inside the cochlear partition. *J. Acoust. Soc. Am.* 24:72–76.
37. O Maoiléidigh, D., and A. J. Hudspeth, 2013. Effects of cochlear loading on the motility of active outer hair cells. *Proc. Natl. Acad. Sci. USA* 110:5474–5479.
38. Iwasa, K. H., 2016. Energy Output from a Single Outer Hair Cell. *Biophys. J.* 111:2500–2511. <http://dx.doi.org/10.1016/j.bpj.2016.10.021>.

39. Liu, Y., S. M. Gracewski, and J.-H. Nam, 2017. Two passive mechanical conditions modulate power generation by the outer hair cells. *PLoS Comp Biol* 13:e1005701.
40. Rabbitt, R. D., 2020. The cochlear outer hair cell speed paradox. *Proc Natl Acad Sci U S A* 117:21880–21888.
41. Cole, K. S., 1968. Membranes, ions, and impulses. University of California Press, Berkely, CA.
42. Santos-Sacchi, J., S. Kakehata, and S. Takahashi, 1998. Effects of membrane potential on the voltage dependence of motility-related charge in outer hair cells of the guinea-pig. *J Physiol* 510 (Pt 1):225–235.
43. Zheng, J., W. Shen, D. Z.-Z. He, K. B. Long, L. D. Madison, and P. Dallos, 2000. Prestin is the motor protein of cochlear outer hair cells. *Nature* 405:149–155.
44. Gale, J. E., and J. F. Ashmore, 1997. An intrinsic frequency limit to the cochlear amplifier. *Nature* 389:63–66.
45. Iwasa, K. H., 1993. Effect of stress on the membrane capacitance of the auditory outer hair cell. *Biophys. J.* 65:492–498.
46. Gale, J. E., and J. F. Ashmore, 1994. Charge displacement induced by rapid stretch in the basolateral membrane of the guinea-pig outer hair cell. *Proc. Roy. Soc. (Lond.) B Biol. Sci.* 255:233–249.
47. Dong, X. X., M. Ospeck, and K. H. Iwasa, 2002. Piezoelectric reciprocal relationship of the membrane motor in the cochlear outer hair cell. *Biophys. J.* 82:1254–1259.
48. Beurg, M., X. Tan, and R. Fettiplace, 2013. A prestin motor in chicken auditory hair cells: active force generation in a nonmammalian species. *Neuron* 79:69–81. <http://dx.doi.org/10.1016/j.neuron.2013.05.018>.
49. Hirokawa, N., 1978. The ultrastructure of the basilar papilla of the chick. *J Comp Neurol* 181:361–374. <http://dx.doi.org/10.1002/cne.901810208>.
50. Mann, Z. personal communication.
51. Dooling, R. J., B. Lohr, and M. L. Dent, 2000. Hearing in birds and reptiles. In R. J. Dooling, R. R. Faye, and A. N. Popper, editors, *Comparative Hearing: Birds and Reptiles*, Springer, New York, NY, 308–359.
52. Fischer, F. P., 1994. Quantitative TEM analysis of the barn owl basilar papilla. *Hearing Res.* 73:1–15.

- 53. Pujol, R., M. Lenoir, S. Ladrech, F. Tribillac, and G. Rebillard, 1992. Correlation between the length of outer hair cells and the frequency coding of the cochlea. *In* Y. Cazals, L. Demany, and K. Horner, editors, Auditory Physiology and Perception, Pergamon Press, 45–52.
- 54. Beurg, M., W. Xiong, B. Zhao, U. Müller, and R. Fettiplace, 2015. Subunit determination of the conductance of hair-cell mechanotransducer channels. *Proc. Natl. Acad. Sci. USA* 112:1589–1594.